Development of Active Matrix Biosensor Array for Cell Screening

Xiaoqiu Huang[1]
I. Nausieda
David W. Greve[2]
(dg07@andrew.cmu.edu)
Department of Electrical and Computer Engineering
Carnegie Mellon University, Pittsburgh, PA 15213

Michael M. Domach
Duc Nguyen
(md0q@andrew.cmu.edu)
(dnguyen@andrew.cmu.edu)
Department of Chemical Engineering
Carnegie Mellon University, Pittsburgh, PA 15213

Abstract
Measurements of the AC electrode impedance can be used to sense changes in cell adhesion to the electrode and also the cell response to drugs. In this paper, we report progress toward the further development of this sensing technology. We describe extended (~ 72 hr) studies of the impedance changes of electrodes which monitor the cell growth under environmentally controlled conditions, and we contrast the signatures of the mouse fibroblast 3T3 and human colorectal carcinoma HCT-116 cell lines. We also describe the design and fabrication of a CMOS-based active matrix sensor array for statistical analysis of a large population of individual cells.

Keywords
cell sensing, electrode, impedance, array

INTRODUCTION
Impedance-based microelectrode sensor arrays are potentially useful for performing drug screening experiments and also for studies of cell adhesion and micromotion. Impedance measurements of electrodes in cell growth medium were first used to study cell behavior by Giaever and his coworkers in 1986 [1]. Briefly, in this sensor one measures the impedance between two electrodes, a larger counterelectrode and a small sensing electrode. When cells are cultured on the electrodes the measured AC impedance changes in a way which depends on the measurement frequency, the cell coverage, and the cell-electrode gap. The impedance increases at moderate and high frequencies because the cells block current flow from the covered portion of the electrode [2,3]. At low frequencies the impedance may decrease as a consequence of products of cell metabolism which accumulate on the electrode surface, altering the surface chemistry.

We are developing arrays of cell-sensing electrodes which can be used to monitor many individual cells or many individual clusters. In the following, we first present the results of long-term studies of the growth of human cancer cells on large electrodes. When compared with previously published measurements on mouse fibroblasts [4], these experiments show that different cell types have clearly distinguishable behavior even for large electrodes. We then report the fabrication and characterization of an active matrix-addressed array of small sensing electrodes which can be used to investigate individual cells.

CELL GROWTH STUDIES
Figure 1 shows the electrode array used in these experiments. There are nine measuring electrodes between 0.015 mm^2 and 0.02 mm^2 in exposed area. The electrodes are sputtered gold with a chromium adhesion layer and are fabricated on a fused silica substrate. Measurements of the impedance magnitude as a function of frequency were performed using an HP 4192A impedance meter which was switched to individual electrodes under computer control. Impedance measurements were made over the frequency range 100 Hz- 1 MHz.

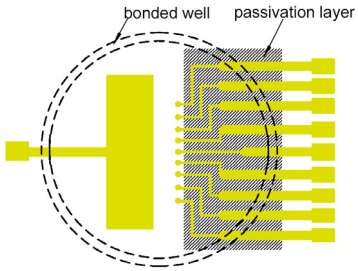

Figure 1. Top view of nine-electrode array. A plastic well was bonded to the substrate to contain the cell growth medium.

Cell growth studies were performed in a controlled environment (T = 37 ºC, 5% CO_2) using Dulbecco's modification of Eagle's medium for fibroblast cells and McCoy's 5A medium for cancer cells. After performing impedance measurements without cells, human cancer cells (HCT-116) were introduced. Figure 2 shows the measured normalized impedance change $r = (Z_{cell} - Z_{no\ cell})/Z_{no\ cell}$ as a function of frequency.

---

[1] Presently with Freescale Semi Inc., 6501 William Cannon Drive West, Austin, TX 78735.
[2] Corresponding author.

In Fig. 2, the peak at approximately 100 kHz is characteristic of cell growth on the electrode [3]. Modeling [2,3] and analysis using the approximate equivalent circuit with and without cells [5] show that the peak height increases with the fraction of the electrode area covered by cells. We observe that the peak height increases with growth time. The peak height appears to saturate near t = 20 hr but increases again between 24 and 48 hours. Also visible is a distinct shift in the peak frequency to lower frequencies as growth proceeds.

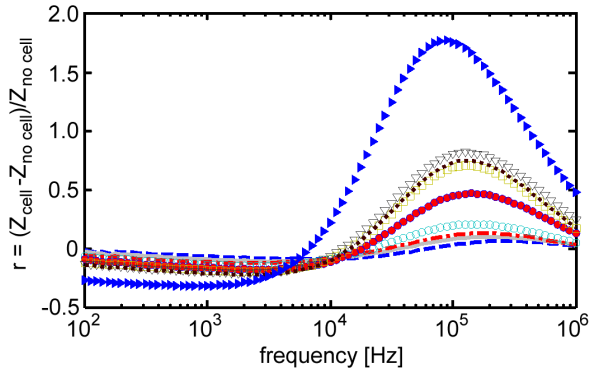

Figure 2. Normalized impedance change *r* as a function of frequency for HCT-116 cells: - - 15 min, – 2 hr, ▪ ▪ ▪ 4 hr, ○ 6 hr, ● 10 hr, □ 14 hr, ▽ 20 hr, ▪ ▪ ▪ 24 hr, and ▶ 48 hr after introduction of cells.

For a single cell, it can be shown that the peak frequency depends on the cell size r_{cell} and the cell-electrode gap t according to $f_{\max} \propto (t/\rho r_{cell}^2)^{1/n}$ where r is the resistivity of the cell growth medium and n is between 0.5 and 1. For the present case where there are many cells forming a layer rcell should be replaced by the the colony size. Consequently the decrease in f_{max} is consistent with the formation of larger colonies, closer cell-electrode spacing, or both.

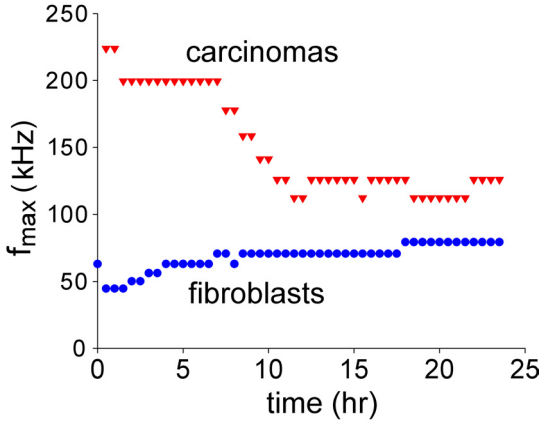

Figure 3. Peak frequency f_{max} as a function of time for human cancer cells (▼) and mouse fibroblasts (●).

This behavior observed for cancer cells is distinctly different from that observed for 3T3 mouse fibroblasts. In contrast to the cancer cells, mouse fibroblasts are contact-inhibited, that is, cells will not overgrow each other and growth ceases when a confluent monolayer is formed. Figure 3 shows the behavior of f_{max} for both cancer cells and mouse fibroblasts. For fibroblasts the peak frequency is lower (consistent with the somewhat larger cell size) and tends to increase rather than decrease with time.

Figure 4 shows the behavior of r_{max} for cancer cells over a longer time period. We clearly observe saturation of r_{max} at approximately 20 hr which corresponds to the formation of a confluent monolayer by microscope observations. Beginning at 30 hr r_{max} begins to increase again and reaches a second plateau at about 45 hours. At the end of this period multiple layers of cells can be observed microscopically.

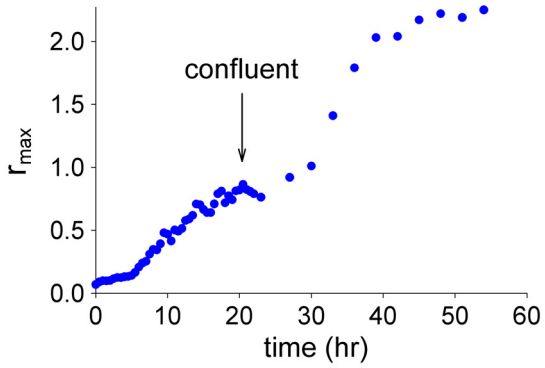

Figure 4 Peak height r_{max} as a function of time for human cancer cells. Microscope observations showed that the cell layer confluent at t = 20 hr.

This impedance changes caused by cancer cells are distinctly different from that previously reported for mouse fibroblasts [4]. Fibroblasts show a sharp increase in rmax between 0 and 6 hr, followed by a decrease in r_{max} as the cells contract in area, and finally a steady increase in rmax between 24 and 65 hr. Table I summarizes the observed behavior of the two cell types. There are clear differences between the cells in the behavior of rmax and also the frequency at which this peak is observed f_{max} . These differences are consistent with the known behavior of these cells.

Table I. Comparison of the electrode impedance changes caused by mouse fibroblasts and human cancer cells.

cell line	spreading time	f_{max} (value)	f_{max} (change)	r_{max} (change)
3T3	~5 hr	< 10^5 Hz	↑	rapid increase, lag, then slow increase
HCT-116	~10 hr	1.3- 2.0 ×10^5 Hz	↓	slow increase, plateau, then slow increase

These results suggest the possibility of distinguishing between cells with different behavior based on the observed behavior of electrode impedance as a function of time. However, the electrodes used in the studies described above are large compared to the cell size and consequently only the average behavior of an ensemble of cells is ob-

served. Smaller electrodes would make it possible to monitor the behavior of individual cells, possibly even making it possible to observe micromotion which is reported to be significantly different for cancer and non-cancer cells [6,7]. Of course one wishes to monitor the behavior of many individual cells in order to obtain statistically significant results. In the following, we will report the fabrication of arrays of cell-sized, individually addressable electrodes.

ACTIVE-MATRIX ELECTRODE ARRAYS

There are three possible approaches for fabrication of an array of sensing electrodes. In the simplest approach each electrode is individually accessed with one interconnect line per electrode. This approach leads to a very large number of contacts and in addition it can be very difficult to route lines from the inside of the array. Superior approaches use row and column lines to access sensing sites located at each crosspoint. Giaever and Keese [8] have used a *passive matrix* array of sensing sites. However passive-matrix addressed arrays have "sneak paths" and as a result the measured impedance can be partly influenced by the impedance of non-selected sites. Here we consider an *active matrix*-addressed array which offers the greatest potential for large arrays.

Figure 5 shows the schematic diagram of an active-matrix addressed array of sensors. Each sensing site is addressed by a normally-off NMOS field effect transistor. One column is selected by driving the column line high with the output of a decoder. The impedance of a single site is measured between one selected row line and a reference electrode.

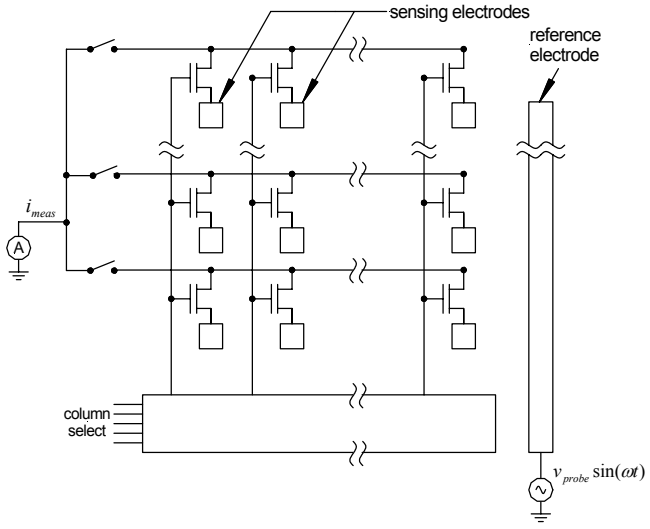

Figure 5. Schematic diagram of an active matrix-addressed array of sensing electrodes.

We have fabricated an array with 120 sensing sites using the AMIS 1.5 micron technology available through MOSIS. The chip is 2 mm × 2 mm in size, with 50 μm × 50 μm sensing electrodes consisting of second-layer metal exposed using the passivation mask. Postprocessing as described below is required to coat the exposed aluminum with gold for biocompatibility and also to protect the bond pads from exposure to the cell growth medium. A CAD layout of the chip is shown in Fig. 6, and a cross section of one sensing site is shown in Fig. 7.

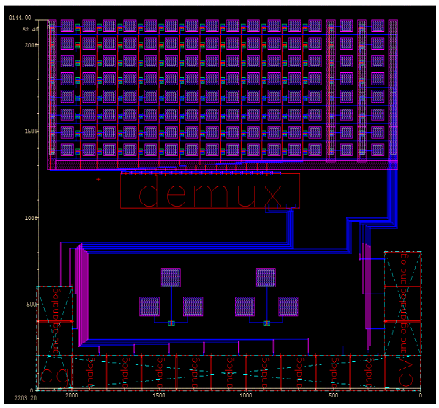

Figure 6. CAD layout of the chip. The active-matrix addressed electrodes are at the top and the decoder and the bond pads are at the bottom.

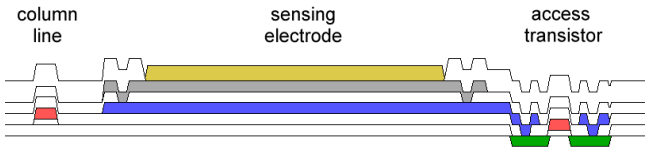

Figure 7. Cross section of a single active-matrix addressed sensing site. The sensing electrode is gold electroless-plated onto second layer metal.

Postprocessing of the fabricated chip is required in order to provide for biocompatible gold electrodes and also to arrange for protection of the bond pads and bond wires. Figure 8a shows the final packaged chip. The chip bond pads and sensing sites are selectively coated with gold using an electroless process described by [9]. The plating process is a multi-step process which includes a surface etch of the aluminum, zincation, desmutting, electroless nickel plating and finally gold plating. Good results are obtained as shown in Fig. 8b provided the chips are processed as bare (unpackaged) chips. Applying the same process to packaged chips results in some unplated electrodes and also some etching of exposed aluminum due to the formation of electrochemical couples with the package metallization.

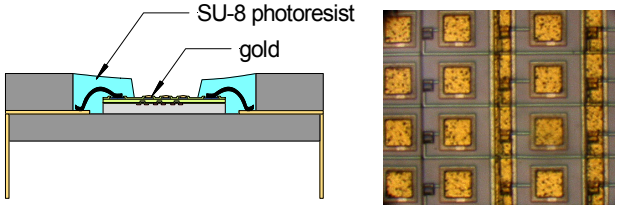

Figure 8. Post-processed chip: (a) in ceramic package showing SU-8 photoresist protecting bond pads and aluminum bond wires, and (b) photograph of chip after elec-

troless gold plating. All exposed aluminum areas are plated with gold.

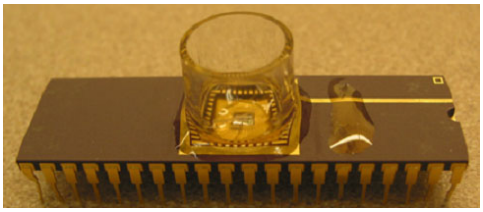

Figure 9. Photograph of completed chip in ceramic package with well for containment of growth medium attached.

The metallized chips were attached to a 40 pin ceramic package using silver epoxy and connections are made using aluminum ultrasonic bonding. Then thick SU-8 photoresist was used to passivate the bond pads and wires. Finally a well was attached for containment of the growth medium. The packaged chip is shown in Fig. 9. The postprocessing approach used here requires only one photolithographic step and that requires only coarse alignment.

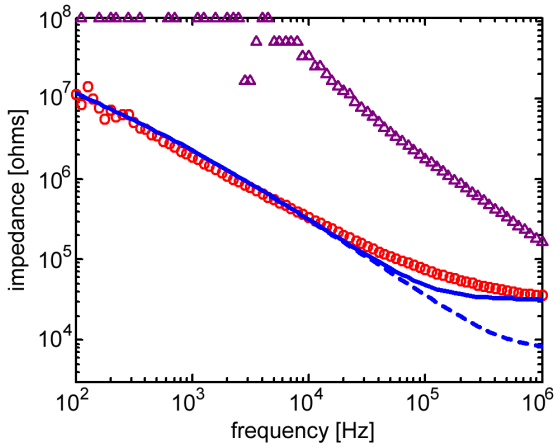

Figure 10. Measured impedance of 50 μm × 50 μm electrode: (△) with addressing transistor off (V_g = -1 V; (○) with addressing transistor on (V_g = 5 V); magnitude of predicted impedance of electrode (--) and simulated impedance using extracted transistor parameters (—).

Operation of the chip is demonstrated in Fig. 10, which compares the measured impedance as a function of frequency with all access transistors turned off and with a single transistor turned on. The measured impedance with the access transistor turned on is compared with the impedance expected for the electrode size. There is very good agreement except at high frequencies where the ON resistance of the access transistor is comparable to the electrode impedance. With the access transistor turned off, the measured impedance is considerably increased.

Biological experiments have not yet been performed using the active matrix arrays. However the results reported here show that relatively simple post-processing can be used to fabricate working arrays. Future work will be directed at studies of single cells on these arrays.

SUMMARY

We have shown that electrode impedance measurements reveal clear differences in the behavior of different kinds of cells even when large electrodes are used. We have therefore developed arrays of electrodes which are small enough to provide measurement of a single cell. We have shown that such arrays can be fabricated from standard CMOS chips by relatively non-critical post-processing, and the operation of fabricated arrays has been successfully demonstrated.

ACKNOWLEDGMENTS

This material is based upon work supported by the National Science Foundation under Grant No. ECS-0088520. Any opinions, findings, and conclusions or recommendations expressed in this material are those of the authors and do not necessarily reflect the views of the National Science Foundation.

REFERENCE

[1] I. Giaever and C.R. Keese, IEEE Transactions on Biomedical Engineering BME-33, pp. 242-247 (1986).

[2] Giaever, I. and Keese, C.R., "Micromotion of mammalian cells measured electrically," Proc. Natl. Acad. Sci., vol. 88, pp. 7896-7900 (1991).

[3] X. Huang, D. Nguyen, D.W. Greve, and M.M. Domach, "Simulation of microelectrode impedance changes due to cell growth," IEEE Sensors vol. 4, pp. 576-583, October, 2004.

[4] X. Huang, D.W. Greve, I. Nausieda, D. Nguyen, and M.M. Domach, "Impedance-based Biosensors," Proceedings of the MRS Spring Meeting, San Francisco, CA, April, 2004 (to be published).

[5] X Huang, "Impedance-based biosensor arrays," unpublished Ph.D. thesis, Department of ECE, Carnegie Mellon University (2004).

[6] A.W. Partin, J.T. Isaacs, B. Treiger and D.S. Coffey, "Early cell motility changes associated with an increase in metastatic ability in rat prostatic cancer cells transfected with the v-Harvey-ras oncogene," Cancer Research vol. 48(21), pp. 6050-3 (1988).

[7] E.M. Posadas, S.R. Criley, and D.S. Coffey, "Chaotic oscillations in cultured cells: rat prostate cancer," Cancer Research 56(16) pp. 3682-8 (1996).

[8] I. Giaever and C.R. Keese , "Cell substrate electrical impedance sensor with multiple electrode array," US patent 5,187,096 (1993).

[9] M. Datta, S.A. Merritt, and M. Dagenais, "Electroless remetallization of aluminum bond pads on CMOS driver chip for flip-chip attachment to vertical cavity surface emitting lasers (VCSELs)," IEEE Trans. Components and Packaging Technology vol. 22, pp. 299-306 (1999).